Research Square

Preprints are preliminary reports that have not undergone peer review.
They should not be considered conclusive, used to inform clinical practice,
or referenced by the media as validated information.

Synergistic Antifungal Efficacy and Enzymatic Mechanisms of Bacillus amyloliquefaciens gfj-4 Extract Combined with fungicides Against Corn Curvularia Leaf Spot

Xingyu Liu
Anhui Science and Technology University
Yuxun Hua
Anhui Science and Technology University
Meng Wang
Anhui Science and Technology University
haiming duan
duanhm@ahstu.edu.cn
Anhui Science and Technology University
Li Yu
Anhui Science and Technology University
Zhuangzhuang Li
Anhui Science and Technology University
Xinyu He
Anhui Science and Technology University
Haibing Yu
Anhui Science and Technology University

Research Article

Keywords: Curvularia lunata, enzymatic mechanism, Microbial metabolites, Synergistic chemical control, maize disease control

Posted Date: May 28th, 2026

DOI: https://doi.org/10.21203/rs.3.rs-9760198/v1

License: This work is licensed under a Creative Commons Attribution 4.0 International License.
Read Full License

Version of Record: A version of this preprint was published at European Journal of Plant Pathology on August 31st, 2026. See the published version at https://doi.org/10.1007/s10658-026-03306-2.

Abstract

Corn *Curvularia* Leaf Spot (CCLS), caused by *C. lunata*, severely impairs corn yield and grain quality. This study investigated the combined efficacy of microbial metabolites from *B. amyloliquefaciens* gfj-4 with chemical fungicides pyraclostrobin and captan for CCLS management, using in vitro toxicity assays and pot experiments to evaluate control performance and synergistic interactions. The strain gfj-4 inhibited *C. lunata* by 73.58%, with its crude extract showing an EC_{50} of 50.18 μg mL^{-1}, while pyraclostrobin and captan exhibited EC_{50} values of 1.56 mg $L^{-1}$and 9.11 mg L^{-1}, correspondingly. Optimal synergistic ratios were 7:3 (crude extract: pyraclostrobin, toxicity ratio = 1.34) and 8:2 (crude extract: captan, toxicity ratio = 1.17), with Wadley formula-derived SR values of 3.70 and 2.48. At 32 h post-treatment, both synergistic agents altered *C. lunata* mycelial SOD(Superoxide dismutase), POD(Peroxidase), soluble protein, and reducing sugar levels, while MDA(Malondialdehyde) content increased over time to a 32 h peak. These optimal combinations achieve sustainable CCLS control via a synergistic "biological enhancement + chemical reduction" strategy, offering theoretical and practical support for eco- friendly disease management.

Introduction

Maize is a crucial global crop for food security, but changes in cultivation practices, like continuous maize growth and straw-returning methods, have altered field conditions (Erenstein et al., 2022). This has led to increased risk of soil-borne diseases due to the accumulation of plant residues, providing habitats for pathogens (Zhang et al., 2022). Corn *Curvularia* leaf spot (CCLS), caused by *C. lunata*, has become more prevalent. The fungus spreads through air-borne conidia, causing severe damage by rapidly expanding lesions and necrosis on leaves (Moparthi et al., 2023). The spread of pathogens and frequent disease outbreaks in modern farming, together with pathogen reservoirs, have increased disease incidence and severity in major corn-producing areas across the globe(Gao et al., 2014). Disease control has traditionally relied on fungicides like triazoles, strobilurins, imidazoles, and other categories (Guilherme et al., 2023). However, due to pathogen resistance, environmental residues, and concerns about non-target organisms, research is focusing on sustainable disease management.

Biological control is an important approach in plant disease management due to its eco-friendliness and ability to reduce pathogen resistance risk (Yue et al., 2025). As a key biocontrol agent, *B. amyloliquefaciens* exerts antagonistic effects against various plant-pathogenic fungi via nutrient competition, antimicrobial compound secretion (Zouari et al., 2016). Its strains and fermentation products achieve over 50% control efficacy against wheat blast and 55%-70% against tomato gray mold (Chen et al., 2019; Jamal et al., 2017). In vitro, multiple biocontrol agents exhibit strong antagonistic activity against *C. lunata*. The mycelial inhibition rate of *Bacillus atrophaeus* SM3 was 93.4%, and that of *Alcaligenes* sp. reached 89.0% (Korany et al., 2023; Rawat et al., 2025). However, unstable field efficacy and slow action of biocontrol preparations limit their popularization.

Combining biocontrol agents with chemical fungicides compensates for the shortcomings of single methods and reduces pesticide use. Xu et al. (2022) confirmed that difenoconazole combined with biocontrol agent SDTB009 achieves both rapid chemical control and sustained biological protection, effectively suppressing tomato Fusarium wilt and providing a new idea for green disease management. Research on combining *B. amyloliquefaciens* with chemical fungicides has primarily focused on rice sheath blight and cucumber powdery mildew, neglecting studies on CCLS. The efficacy of microbial metabolites from fermentation broths and their synergistic effects with fungicides, including optimal ratios, lack thorough evaluation. Furthermore, mechanistic understanding of their combined disease control is inadequate, particularly regarding effects on pathogen morphology and enzymatic activities. Knowledge gaps impede the translation of collaborative control technologies from lab to field, necessitating systematic research. Different from the studies only focusing on the efficacy of single biocontrol agents or single chemical fungicides, this study innovatively conducts the screening of synergistic combinations between the crude extract of *B. amyloliquefaciens* gfj-4 fermentation broth and chemical fungicides, determines the optimal synergistic ratio, further analyzes the antibacterial mechanism of the combined system from the physiological and biochemical perspective of pathogens, constructs a bio-chemical synergistic green prevention and control scheme, realizes the reduction and efficiency of fungicides, and provides new ideas and experimental support for the green prevention and control of corn curved leaf spot disease. This study utilized fermentation metabolites from *B. amyloliquefaciens* gfj-4 in combination with 12 chemical fungicides to combat CCLS effectively and sustainably.

Material and Methods

Fungicides, Pathogenic Fungi, Antagonistic Bacteria, Culture Media and Corn Varieties

The technical-grade fungicides supplied were prochloraz (96.0%), tebuconazole (96.0%), propiconazole (95.7%), hexaconazole (95.0%), epoxiconazole (96.0%), pyraclostrobin (97.5%), trifloxystrobin (97.5%), fludioxonil (98.0%), myclobutanil (96.0%), captan (95.0%), bromothalonil (95.0%), and procymidone (50.0%) wettable powder from Jiangsu Fengdeng Crop Protection Co., LTD. *C. lunata* (Wakker) Boed., *B. amyloliquefaciens* strain gfj-4, and *C. lunata*-susceptible corn inbred line 73A were maintained in the laboratory. Media used were Nutrient broth (NB), Potato dextrose agar (PDA) and Nutrient agar (NA) (Luo et al., 2024)

Inhibitory Effect of B. amyloliquefaciens gfj-4 on C. lunata determined by the dual culture

The dual culture method described by Li et al. (2023) was employed. Circular filter paper discs (Φ = 7 mm) were positioned around the pathogen in a cross pattern, 5 cm apart and equidistant from the central inoculum (7 mm agar plug of 4-day-old *C. lunata*). *B. amyloliquefaciens* strain gfj-4 culture (2 μL) was pipetted onto each disc. The experiment was triplicated, meanwhile, the sterile water was served as

control. Incubation occurred at 26°C in a constant temperature-humidity incubator for 96 h. Colony growth inhibition rate was calculated following He et al. (2025).

Inhibition Activity of the Fermentation Metabolites and 12 Fungicides Against C. lunata

Fermentation metabolites were obtained via the protocol described by Jiao et al. (2021) at a concentration of 8.0×10^5 mg L^{-1}. Antifungal activity was assessed by means of the mycelial growth rate method as reported by Huang et al. (2024). Different concentrations of the crude extract and various fungicides were prepared by dilution in PDA medium. Pathogenic fungal mycelial plugs were placed on the PDA plates, followed by incubation at 26°C for 96 h. After incubation, colony diameters were measured to compute the EC_{50}, toxicity regression equation, and R^2 for each individual treatment group (Table 1).

Table 1
Concentration gradient of 12 chemical fungicides.

Fungicide	Concentration series (mg L^{-1})					
Fludioxoni	0.01	0.04	0.08	0.16	0.24	0.32
Prochloraz	0.05	0.10	0.20	0.40	0.80	1.60
Epoxiconazole	0.10	0.20	0.40	0.80	1.60	3.20
Tebuconazole	0.10	0.20	0.40	0.80	1.60	3.20
Propiconazole	0.13	0.25	0.50	1.00	2.00	4.00
Hexaconazole	0.05	0.10	0.20	0.40	0.80	1.60
Myclobutanil	0.10	0.20	0.40	0.80	1.60	3.20
Procymidone	0.25	0.50	1.00	2.00	4.00	8.00
Pyraclostrobin	0.20	0.40	0.80	1.60	3.20	6.40
Trifloxystrobin	1.00	2.00	4.00	8.00	16.00	24.00
Bromothalonil	1.00	2.00	4.00	8.00	16.00	32.00
Captan	1.00	2.00	4.00	8.00	16.00	32.00

Synergistic Effect of Fermentation Broth-Derived Crude Extract with Chemical Fungicides

The Horsfall method was adopted to determine the toxicity ratios of fermentation broth crude extract combined with chemical fungicides against *C. lunata*. Eleven distinct volume ratios were set up, with sterile water as the control (Horsfall J.G., 1945). For these extract-fungicide combinations, the toxicity

regression equation, EC_{50} value, R^2 coefficient, and synergistic ratio (SR) were calculated using the Wadley formula (Wadley F.M., 1967).

Inhibitory Effect of Synergistic Combinations on the Colonization of C. lunata on Detached Corn Leaves

Preliminary toxicity tests were conducted to determine the EC_{50} and EC_{80} values of *Bacillus amyloliquefaciens* gfj-4 crude extract and tested fungicides against *Curvularia lunata*. According to the optimal concentration selection criteria for combined application research (Ons et al., 2020), EC_{80} was selected to evaluate agent interaction and synergistic effects, which could avoid the ceiling effect at EC_{90} and insufficient antifungal activity at EC_{50}. Panicle leaves from corn inbred line 73A were selected for uniform growth and intact blades. After thorough cleaning and air-drying, the leaves were subjected to three individual treatments at their respective EC_{80} concentrations: the crude fermentation broth extract (EC_{80} = 257.1 mg L^{-1}), pyraclostrobin (EC_{80}= 10.53 mg L^{-1}), and captan (EC_{80}= 58.40 mg L^{-1}). For the combined treatments, the optimal mass ratios were pre-determined as 75.06:1 for the crude extract mixed with pyraclostrobin, and 22.03:1 for the crude extract combined with captan. The corn leaves were soaked in 200 mL solutions for 30 seconds, then exposed to *C. lunata* mycelial plugs. After 4 d, lesion sizes were assessed to determine inhibition rates (Lee et al., 2023).

Control Efficacy of the Optimal Synergistic Combination Against CCLS by Pot Experiments

Corn kernels of the 73A variety were germinated in sterile water. Four germinated seeds were planted individually in pots with commercial seedling substrate. Two healthy seedlings were kept in each pot (16.0 cm in diameter, 14.0 cm in height) after emergence. The experiments began when the seedlings reached the three-leaf and one-heart stage.

: For the preventive treatment group, corn seedlings were sprayed with the crude extract, pyraclostrobin, and captan at their respective EC_{80} concentrations of 257.1 mg L^{-1}, 10.53 mg L^{-1}, and 58.40 mg L^{-1}. The crude extract was blended with pyraclostrobin at a mass ratio of 75.06:1 and with captan at a mass ratio of 22.03:1. Plants were then transferred to a controlled environment with specific light (6000 lux for 10 h) and temperature conditions (24℃ light period, 20℃ dark period; 90% RH). Each treatment was applied to 6 pots and the experiment was repeated 3 times. 12 h post-treatment, a spore suspension of *C. lunata* (10^6 CFU mL^{-1}) was sprayed to inoculate CCLS. Plants were returned to the incubator and monitored until the tenth day to calculate the disease indexes control efficacies based on CCLS grading criteria (Loladze et al., 2019)

: Plants in the treatment group were exposed to a suspension of CCLS pathogen spores at a concentration of 10^6 CFU mL^{-1}, then transferred to a climate chamber set at 90% RH. The chamber had programmed light (6000 lux, 24℃) and dark (20℃) periods, with a 12 h culture interval. Fungicide preparation and incubation conditions matched those of the prevention treatment group.

Effect of the Synergistic Combination on the Cell Membrane Permeability

Mycelial discs of *Curvularia lunata* (causal agent of maize curvularia leaf spot) were inoculated into 500 mL Erlenmeyer flasks containing 300 mL of potato dextrose broth (PDB). After constant-temperature shaking culture, the mycelia were collected, rinsed with sterile water, and filtered to remove residual medium. Cell membrane permeability can be indirectly reflected by the extracellular leakage of intracellular electrolytes, and electrical conductivity measurement is a classic physiological index for evaluating the degree of cell membrane damage in pathogenic fungi (Liu et al., 2024). In this experiment, equal amounts of fresh mycelia were separately exposed to single fungicide solution at the EC_{50} concentration and the optimal synergistic compound solution, with sterile water treatment set as the blank control. All samples were incubated in a shaker at 26 ℃ and 130 r/min. The electrical conductivity of each system was determined at 0, 5, 15, 30, 60, 90, 180, 240 and 360 min after treatment, with three biological replicates for each treatment.

Effects of Synergistic Combinations on Levels of SOD, POD, MDA, Soluble Protein and Reducing Sugar in C. lunata

The EC_{50} concentrations of each agent against *C. lunata* were determined. Liquid formulations were prepared by mixing 10 mL of each agent with 90 mL of PDB medium. The crude extract, pyraclostrobin, and captan reached concentrations of 50.18 mg L^{-1}, 1.56 mg L^{-1}, and 9.11 mg L^{-1}, correspondingly. According to their EC_{50} levels, the ideal ratios for mixing the crude extract with pyraclostrobin and captan were 7:3 and 8:2, in that order. Three grams of mycelium were introduced into the modified PDB solution and placed in a thermostatic shaker at 26℃ and 130 r min^{-1}. Triplicate samples were collected at 0, 4, 8, 16, 24, and 32 h intervals. The mycelium obtained was treated by homogenizing 0.50 g of each sample in phosphate buffer (pH 7.8) within an ice bath.

Samples were centrifuged at 4℃ and 12, 000 r min^{-1} for 20 min. The supernatant was stored at − 20℃ for subsequent analysis of superoxide dismutase (SOD), peroxidase (POD), malondialdehyde (MDA), soluble protein, and reducing sugar. SOD activity was determined at 560 nm using the azadiazole colorimetric method (Cheng et al.,2015). POD activity was assessed at 470 nm with the guaiacol colorimetric method (Zondo et al.,2024). MDA content was measured at 600 nm, 532 nm, and 450 nm using the thiobarbituric acid colorimetric assay (Senthilkumar et al.,2020). Soluble protein was quantified at 595 nm with the Coomassie Brilliant Blue G-250 colorimetric assay (Deans et al.,2018). Reducing sugar was analyzed at 540 nm using the 3,5-dinitrosalicylic acid colorimetric method (Jain et al.,2020).

Data Analysis

Statistical analyses were conducted using SPSS 26.0 software. The EC_{50} of the tested pathogen was calculated via regression analysis between fungicide logarithmic concentration and mycelial growth inhibition rate. All experimental data were first subjected to one-way analysis of variance (ANOVA) to

detect overall significant differences among treatments, and Duncan's multiple range test was further applied for post-hoc multiple comparisons at the significance level of ($p < 0.05$).

Results

Antagonistic Effect of B. amyloliquefaciens gfj-4 Against C. lunata

The co-culture results showed the antagonistic effect of biocontrol strain gfj-4 against *Curvularia lunata* at 96 h after incubation (Figure 1). In the control group, the mycelia of *C. lunata* grew vigorously and fully covered the filter paper. Compared with the control, the application of strain gfj-4 markedly suppressed the vegetative growth of the pathogen, restricted mycelial radial expansion, and the corresponding growth inhibition rate reached 73.58%±2.76%. Notably, inoculation spacing and inoculation patterns are key factors affecting antagonistic performance and inhibition rate calculation. In this experiment, a unified dual-culture inoculation distance was adopted, and the pathogen growth inhibition rate was calculated via colony diameter measurement in accordance with standard antagonistic assay protocols.

Inhibitory Effect of the Crude Extracts and 12 Chemical Fungicides on C. lunata

Increasing the concentration of the crude extract from 25.00 mg L^{-1} to 200.00 mg L^{-1} elevated inhibition rates against *C. lunata* from 30.64% to 71.72% (Table 2). For the crude extract, its EC_{50} was measured at 50.18 mg L^{-1}, and the dose-response regression equation was $y = 1.17x + 3.02$ (R^2=0.95). Treatment with the crude extract led to morphological changes in *C. lunata*, including roughened mycelial surfaces, increased septation, swollen hyphal tips, disordered growth with twisting, invaginations, and fragmentation. Additionally, protoplast concentration within hyphae and conidial production notably increased, suggesting that the inhibitor promoted sporulation in *C. lunata* (Fig. 2).

Table 2
Inhibitory effect of the crude extract on *C. lunata*.

Concentration (mg L^{-1})	Inhibition rate (%) [a]
200.00	71.72 + 1.01 a
100.00	66.67 + 1.54 b
66.67	60.94 ± 0.34 c
50.00	55.89 ± 0.34 d
33.33	42.42 ± 0.02 e
25.00	30.64 ± 1.21 f

[a]:Distinct lowercase letters post data show notable variations in inhibition rates of various concentrations of crude extract against *C. lunata*, as established by Duncan's multiple range test at the 0.05 significance level.

Figure 2 Inhibition effect of the crude extract on *C. lunata*. The **A, B, C, D** and **E** and **F** are 200.00, 100.00, 66.67, 50.00, 33.33 and 25.00 mg L^{-1}, respectively. **G** is the control mycelium of *C. lunata*, and H is the mycelium of *C. lunata* after treatment.

Among all tested fungicides, fludioxonil showed the highest inhibitory activity toward *C. lunata*, corresponding to an EC_{50} of 0.01 mg L^{-1}. Sterol C-14α-demethylase inhibitors were ranked from high to low according to their antifungal activity, with the order being prochloraz (0.12 mg L^{-1}), epoxiconazole (0.20 mg L^{-1}), tebuconazole (0.28 mg L^{-1}), propiconazole (0.34 mg L^{-1}), hexaconazole (0.46 mg L^{-1}) and myclobutanil (0.47 mg L^{-1}). Pyraclostrobin and trifloxystrobin had EC_{50} values of 1.56 mg L^{-1} and 5.94 mg L^{-1}, separately. As for procymidone, bromothalonil and captan, their EC_{50} values were measured to be 0.62, 7.87 and 9.11 mg L^{-1} in sequence. (Table 3).

Table 3
Inhibitory activity of 12 fungicides against *C. lunata*.

Fungicide	Toxicity regression equation [a]	EC_{50} (mg L^{-1})	95% confidence interval (mg L^{-1})	R^2
Fludioxoni	y = 0.78x + 6.45	0.01	0.005–0.02	0.96
Prochloraz	y = 0.77x + 5.71	0.12	0.09–0.15	0.96
Epoxiconazole	y = 1.70x + 6.19	0.20	0.16–0.24	0.95
Tebuconazole	y = 1.17x + 5.64	0.28	0.23–0.34	0.97
Propiconazole	y = 1.34x + 5.63	0.34	0.28–0.40	0.97
Hexaconazole	y = 1.60x + 5.53	0.46	0.40–0.56	0.99
Myclobutanil	y = 0.90x + 5.30	0.47	0.38–0.58	0.95
Procymidone	y = 1.79x + 5.37	0.62	0.54–0.71	0.97
Pyraclostrobin	y = 1.05x + 4.80	1.56	1.30–1.91	0.97
Trifloxystrobin	y = 0.63x + 4.52	5.94	4.23–9.35	0.95
Bromothalonil	y = 1.20x + 3.92	7.87	6.51–9.67	0.96
Captan	y = 1.04x + 4.00	9.11	7.30-11.73	0.97

[a]: x is the log value of how much drug was used, and y is the statistical probability unit derived from the inhibition rate.

Antifungal Effect of the Mixture of Crude Extract and Fungicides

The most significant synergistic inhibitory effect against *C. lunata* occurred by combining the crude extract with pyraclostrobin in a 7:3 ratio and with captan in an 8:2 ratio, resulting in toxicity ratios of 1.34

and 1.17, respectively. Mixtures of the crude extract with bromothalonil, hexaconazole, procymidone, tebuconazole, or fludioxonil also showed synergistic effects under specific proportions (data not shown). Consequently, the combinations with pyraclostrobin and captan were selected for additional experimentation (Fig. 3).

Increasing concentrations of the crude extract and the two fungicides combinations enhanced the inhibition rate of *C. lunata*. At 64.00 mg L^{-1}, the mixture achieved a 78.69% inhibition rate. The mixture's toxicity regression equation was y = 0.95x + 4.06 (R2 = 0.99), yielding a theoretical EC_{50} of 35.99 mg L^{-1} and an observed EC_{50} of 9.73 mg L^{-1}, leading to a synergy ratio (SR) of 3.70. Similarly, the combination of the crude extract and captan at 64.00 mg L^{-1} led to a 77.95% inhibition rate. The regression equation for the mixture's toxicity was y = 1.32x + 3.41 (R^2 = 0.98), yielding a theoretical EC_{50} of 41.97 mg L^{-1} and an observed EC_{50} of 16.90 mg L^{-1}, leading to an SR of 2.48. These findings confirmed the significant synergistic effects of the crude extract when combined with pyraclostrobin and captan (Table 4).

Table 4
Inhibitory effects of crude extract combined with pyraclostrobin and captan at the optimal combination ratio against *C. lunata*.

Combination	**Mixture concentration (mg L^{-1})**	**Inhibition rate (%) [a]**
Crude extract-Pyraclostrobin	4.00	37.05 ± 0.57 f
	8.00	44.26 ± 0.33 e
	16.00	59.67 ± 0.57 d
	24.00	64.26 ± 1.18 c
	32.00	68.20 ± 0.87 b
	64.00	78.69 ± 0.33 a
Crude extract-Captan	8.00	33.85 ± 1.08 f
	16.00	49.38 ± 1.12 e
	24.00	61.80 ± 0.54 d
	32.00	66.46 ± 1.42 c
	48.00	72.98 ± 1.08 b
	64.00	77.95 ± 0.62 a

[a]: Distinct lowercase letters post data show notable variations in the suppression rates of the two combined blends against *C. lunata*, as established by Duncan's multiple range test at the 0.05 significance level.

Antifungal Effect of the Two Synergistic Mixtures on the Isolated Leaves

The crude extract, pyraclostrobin and captan individually inhibited *C. lunata* spread by 44.44%, 48.61% and 41.67%. Combining the crude extract with pyraclostrobin resulted in a 75.69% inhibition rate, surpassing the crude extract by 70.32% and pyraclostrobin by 55.71%. The crude extract with captan inhibited by 66.39%, 49.39% and 59.32% more than the individual treatments. The mixture of the crude extract and pyraclostrobin showed the highest pathogen suppression and improvement over single-agent treatments (Table 5). Overall, combining the crude extract with pyraclostrobin or captan synergistically inhibited *Curvularia* leaf spot on corn leaves.

Table 5
Inhibitory effects of the crude extract combined with pyraclostrobin and captan against CCLS.

Treatment	Inhibition rate (%) [a]
CK	—
Crude extract	44.44 ± 0.09 d
Pyraclostrobin	48.61 ± 0.09 c
Captan	41.67 ± 0.09 e
Crude extract + Pyraclostrobin	75.69 ± 0.22 a
Crude extract + Captan	66.39 ± 0.21 b

[a]: Different lowercase letters following the data indicate significant differences in the inhibition rates of *C. lunata* expansion on detached leaves among different treatments at the 0.05 significance level.

Potted Test of the Synergistic Effect

For CCLS control, the protective and curative efficacies of the crude extract were determined to be 28.92% and 34.80%, respectively. Pyraclostrobin displayed protective and curative efficacies of 39.29% and 40.89%, while captan achieved 39.09% and 35.56%, respectively. Combining the crude extract with captan resulted in 47.54% in protective efficacy, representing increases of 64.38% and 21.62% compared to individual treatments of the crude extract and captan. Similarly, combining the crude extract with pyraclostrobin led to 48.50% control efficacy, with gains of 67.70% and 23.44% versus single agents. Co-administration of the crude extract with captan resulted in a 49.68% curative efficacy, exceeding the single use of each agent by 42.76% and 39.71%. Stimultaneously, the crude extract with pyraclostrobin yielded a curative efficacy of 51.69%, exceeding single-agent efficacies by 48.53% and 26.41% (Table 6). These findings demonstrated the synergistic effects when mixing the crude extract with pyraclostrobin and captan to control corn *Curvularia* leaf spot.

Table 6
Control efficacies of synergistic combinations against CCLS in pot experiment.

Application method	Treatment	Disease index	Control efficacy (%)[a]
Protective treatment	CK	86.79 ± 0.44 a	—
	Crude extract	61.69 ± 0.37 ab	28.92 ± 1.84 c
	Pyraclostrobin	52.69 ± 0.56 b	39.29 ± 1.69 b
	Captan	52.86 ± 0.35 b	39.09 ± 1.48 b
	Crude extract + pyraclostrobin	44.70 ± 0.49 c	48.50 ± 1.35 a
	Crude extract + Captan	45.53 ± 0.28 c	47.54 ± 1.70 a
Curative treatment	CK	83.62 ± 0.29 a	—
	Crude extract	54.52 ± 0.30 b	34.80 ± 1.01 b
	Pyraclostrobin	49.43 ± 0.30 b	40.89 ± 1.01 b
	Captan	53.88 ± 0.25 b	35.56 ± 1.17 b
	Crude extract + pyraclostrobin	40.40 ± 0.17 c	51.69 ± 1.78 a
	Crude extract + Captan	42.08 ± 0.29 c	49.68 ± 1.81 a

[a]: Different lowercase letters following the data indicate significant differences in the disease control efficacy against corn *Curvularia* leaf spot among different treatments at the 0.05 significance level.

Effect of Synergistic Combinations on Cell Membrane Permeability of C. lunata

The electrical conductivity of *C. lunata* mycelium increased over time in all treatments (Fig. 4). Co-application of the crude extract and pyraclostrobin resulted in a greater membrane permeability compared with the separate use of each individual agent. At 360 min, conductivity in the combined treatment was 1.10-fold and 1.06-fold higher than with crude extract and pyraclostrobin alone, respectively. Addtionally, the crude extract and captan synergistically disrupted the pathogen's mycelial membrane. Compared to individual use, their combination increased membrane damage. At 360 min, conductivity in this combined treatment was 1.04-fold and 1.05-fold higher than with the crude extract and captan alone, respectively. Overall, the optimized mixture of the crude extract, pyraclostrobin, and captan caused more severey damage to cell membrane of *C. lunata* than any single treatment, enhancing inhibitory activity against pathogen growth.

Influence of Synergistic Combinations on Mycelial SOD, POD Activities and MDA Content of C. lunata

In the control group, SOD activity in *C. lunata* mycelia was maintained at a stable level, while all other treatments induced a progressive decline in this enzyme activity. At 32 h, mycelia treated with combined formulations showed the lowest SOD activity. For instance, mycelia treated with crude extract-

pyraclostrobin had 76.84 U g^{-1} FW, 37.07% and 29.47% lower than crude extract and pyraclostrobin alone. Mycelia treated with crude extract-captan had 84.74 U g^{-1} FW, 30.60% and 28.76% lower than crude extract and captan alone. These decreases in SOD activity indicated elevated oxidative stress under combined treatments, thereby confirming a synergistic inhibitory effect relative to single-component counterparts. The crude extract–pyraclostrobin combination caused a non-significant initial reduction in POD activity of *C. lunata* mycelia in comparison with other treatments, but this activity plummeted to the minimum value of 3.42 U g^{-1} FW min^{-1} at 32 h, manifesting an obvious synergistic inhibitory effect. For the crude extract–captan combination, POD activity in *C. lunata* mycelia was reduced to 3.62 U g^{-1} FW min^{-1} at 32 h, a 65.05% decrease from the control. These declines in POD activity suggested that synergistic combinations caused more damage to *C. lunata* mycelia than single treatments (Fig. 5).

MDA levels in *C. lunata* mycelia increased over time in all treatment groups, consistently surpassing the control group (Fig. 6). At 32 h, the crude extract–pyraclostrobin combination showed the highest MDA concentration, exceeding the control by 52.58%, the crude extract and pyraclostrobin alone by 33.28% and 27.60%, respectively. The crude extract–captan combination also peaked at 32 h, with MDA levels 45.80% higher than the control, and 23.75% and 20.16% higher than the crude extract and pyraclostrobin alone, respectively. These findings suggested that the synergistic combinations led to a notable MDA accumulation in mycelia, enhancing the inhibitory effect against *C. lunata*.

Effects of Synergistic Combinations on Levels of Soluble Protein and Reducing Sugar in C. lunata

In the control group, soluble protein levels in *C. lunata* mycelia stayed stable, whereas all treatments fluctuated obviously, peaking at 8 h and then decreasing continuously. By 32 h, soluble protein content in every treatment was lower than the control. The crude extract–pyraclostrobin combination recorded 15.30 mg g^{-1} FW soluble protein, 71.89%, 51.44% and 53.92% lower than the control, crude extract alone and pyraclostrobin alone, respectively. The crude extract–captan mixture had 19.18 mg g^{-1} FW, with reductions of 64.76%, 39.13% and 46.11%. The initial protein increase was attributed to adaptive synthesis under inhibitor stress, while prolonged exposure suppressed biosynthesis and caused a sharp decline. Combined treatments showed the lowest protein levels, enhancing antifungal efficacy by impairing protein synthesis. Mycelial reducing sugar contents presented a similar pattern, increasing first and then decreasing, with all treatments peaking at 8 h and exceeding the control. At 32 h, the crude extract–pyraclostrobin combination had 0.44 mg g^{-1} FW reducing sugar, 59.20%, 41.66% and 36.05% lower than the control and two single treatments. The crude extract–captan group had 0.52 mg g^{-1} FW, with corresponding reductions of 51.53%, 30.69% and 29.30%. These results confirmed that combined formulations had significantly lower reducing sugar contents than single treatments, further improving antifungal activity (Fig. 7).

Discussion

C. lunata–induced leaf blight has become a prevalent production disease in major corn-producing regions globally, with escalating incidence and mycotoxin accumulation (Gao et al.,2017). Chemical control is the primary management approach, with effective fungicides identified. Carboxin and mancozeb are potent against *C. lunata*, with carboxin fully inhibiting growth at 25 mg L^{-1} and mancozeb achieving 98.24% inhibition at 200 mg L^{-1} (Bisht et al.,2018) In this study, fludioxonil, prochloraz, epoxiconazole, tebuconazole, propiconazole, hexaconazole, and myclobutanil exhibited strong antifungal effects, notably fludioxonil against *C. lunata*. Chemical fungicides vary in modes of action, affecting their efficacies against *C. lunata*. Tailoring fungicide selection and rates to specific field conditions is crucial for effective management, rather than following a uniform protocol. Surveillance has revealed reduced susceptibility of *C. lunata* to various chemicals, with highly resistant populations in some regions. Even with fungicide rotation, maintaining control is challenging. These findings emphasize the necessity of developing new control strategies to better manage pathogen resistance evolution and spread(Kim et al.,2024).

The evolution of *C. lunata* resistance to chemical fungicides is driven by complex interactions between agricultural practices and pathogen genetic plasticity(Bengyella et al.,2017).Long-term over-reliance on single-site fungicides (e.g., DMIs, QoIs) exerts intense selection pressure, favoring the survival and propagation of resistant mutants（Carmona et al.,2020）. Previous studies have documented that *C. lunata* develops resistance through multiple mechanisms: target-site mutations (e.g., CYP51 gene mutations confer resistance to tebuconazole and propiconazole), overexpression of efflux pump genes that extrude fungicides from cells, and enhanced detoxification of fungicides via cytochrome P450 enzymes (Joe et al., 2025). Notably, resistance to QoI fungicides (e.g., pyraclostrobin) often arises from point mutations in the cytochrome b gene, leading to complete loss of fungicide efficacy. Multi-site fungicides like mancozeb are less prone to resistance due to their non-specific mode of action, but improper application (e.g., sub-lethal doses) can still reduce pathogen susceptibility over time. The emergence of resistant *C. lunata* populations not only reduces the effectiveness of existing chemical control but also increases production costs and environmental risks, making the integration of biocontrol agents a critical strategy to mitigate resistance development. By combining *B. amyloliquefaciens* gfj-4 crude extract with reduced doses of chemical fungicides, we can lower the selection pressure on *C. lunata*, slow the rate of resistance evolution, and extend the service life of valuable fungicide resources.

Chanworawit et al. (2023) isolated *B. thuringiensis* and *Paenibacillus* sp. from the termite-gut microbiome, both inhibiting *C. lunata* growth by 29.0% to 72.0%. Xie et al. (2020) observed that volatile organic compounds (VOCs) from *B. subtilis* DZSY21 suppressed *C. lunata* growth by 36.2%. Saleem et al. (2002) reported *Bacillus* sp. strain BC121 reduced *C. lunata* hyphae by 60.0%. Intriguingly, *B. amyloliquefaciens* gfj-4 significantly inhibited *C. lunata* growth by 73.58% in dual-culture assays, with an EC_{50} of 50.18 μg mL^{-1}, which displayed potent antagonistic effects surpassing previous studies. The study suggested that *B. amyloliquefaciens* gfj-4 showed the promise as a biocontrol agent. Despite the benefits of biological control, its application in agriculture is hindered by challenges such as poor storage stability and susceptibility to environmental factors.

Screening synergistic fungicide combinations is crucial for enhancing plant disease management(Maria et al.,2024). Studies on CCLS had demonstrated the effectiveness of mixed-formulation treatments. For instance, Hao et al. (2020) identified potent antifungal activity in pairings like propiconazole-azoxystrobin, trifloxystrobin-tebuconazole, pyraclostrobin-epoxiconazole, and kresoxim-methyl-epoxiconazole. Adaangadi et al. (2018) also found success with carboxin-thiram, captan-hexaconazole, and pyraclostrobin·epoxiconazole against *C. lunata*. Unlike traditional approaches isolating chemical formulations, this research explored the synergistic effects of *B. amyloliquefaciens* gfj-4 crude extract combined with fungicides. The results indicated that incorporating this microbial extract can reduce fungicide dosage without compromising the disease control effect, thus mitigating environmental risks linked to pesticide use. Wang et al. (2024) identified that mixing *B. amyloliquefaciens* gfj-4 crude extract with pyraclostrobin at a volume ratio of 8:2 conferred high activity against Northern Corn Leaf Blight (NLBC). Our study confirmed this ratio's synergistic impact on CCLS, highlighting its broad utility. Additionally, we discovered a synergistic blend of strain gfj-4 extract with captan, expanding biocontrol strategies. The core idea of combining biocontrol agents with reduced chemical use presents a practical approach to disease management. This strategy mirrors the resistance-management model seen in Brazil in 2023, where "Trichoderma + halving of QoI fungicides" was successfully implemented (Brito et al.,2020).

The cell membrane is crucial for a cell's viability (Wolkers et al.,2018). This study showed that a synergistic agent increased electrical conductivity around *C. lunata* mycelium, leading to higher MDA levels and lipid peroxidation, indicating cell membrane damage. This aligned with previous research on *Streptomyces hygroscopicus* subsp. *hygroscopicus* extract causing irreversible membrane damage in banana wilt pathogen (Yun et al., 2023). The synergistic agent impaired *C. lunata*'s antioxidant defenses by reducing SOD and POD activities after 32 h of treatment. This inhibition can lead to ROS accumulation, causing oxidative damage to various cell components. Earlier studies by Yang et al. (2024) and Chen et al. (2020) have also illustrated how antifungal agents impair antioxidant enzymes, resulting in ROS accumulation and subsequent cellular damage. This shared mechanism highlights the importance of perturbing the antioxidant system and ROS homeostasis to target pathogenic cells. Under stress, *C. lunata* mycelium showed a rise-fall pattern in soluble protein and reducing-sugar levels. Initially, levels increased due to stress responses and energy accumulation. Subsequently, a sharp decline indicated inhibition of essential metabolite synthesis, worsening metabolic dysfunction. The compound's synergistic inhibition likely stemmed from disruptions to cell membrane, antioxidants, and metabolic pathways, forming the primary mechanism against *C. lunata*. Beyond the mechanistic insights, the synergistic combinations identified in this study hold significant potential for field application, addressing the practical limitations of single chemical or biological control. The 8:2 volume ratio of *B. amyloliquefaciens* gfj-4 crude extract to pyraclostrobin, and the novel combination with captan, offer dual advantages: reducing chemical fungicide dosage by 40–50% compared to single chemical applications, while enhancing the stability and efficacy of the biocontrol component. In field settings, the chemical fungicide component provides rapid initial control of *C. lunata*, suppressing acute infection, while the microbial extract sustains long-term suppression by inhibiting conidial germination and mycelial growth,

forming a complementary protective effect. This combination also mitigates the environmental sensitivity of *B. amyloliquefaciens* gfj-4, as the chemical fungicide creates a more stable microenvironment for the microbial metabolites to exert their activity. Furthermore, reduced fungicide dosage minimizes residual accumulation in soil and corn grains, complying with green agricultural standards and reducing risks to non-target organisms such as beneficial soil microbes and pollinators(Khaskheli et al., 2025). To maximize field efficacy, future studies should optimize the formulation of the synergistic mixture—for example, adding stabilizers to extend the storage life of the crude extract and adjusting application timing to coincide with the early stages of *C. lunata* infection (e.g., seedling stage or before the onset of leaf blight symptoms). Additionally, evaluating the mixture's performance under diverse ecological conditions (e.g., varying soil types, temperature, and humidity) across major corn-producing regions will validate its broad adaptability. Long-term field trials are also needed to monitor its impact on *C. lunata* resistance evolution, ensuring the sustainability of this control strategy. Future studies should assess the novel mixture's performance in the field and explore its molecular-level synergistic mechanisms.

Conclusion

Bacillus amyloliquefaciens gfj-4 exhibited a significant inhibitory effect against *Curvularia lunata*, the causal agent of maize *curvularia* leaf spot, with an inhibition rate of 73.58% in dual culture assays. Toxicity bioassays of the crude extract of fermentation broth and two chemical fungicides against the pathogen revealed that the EC_{50} value of the crude extract was 50.18 mg/L, while those of pyraclostrobin and captan were 1.56 mg L and 9.11 mg L, respectively. To investigate the synergistic interaction of the combined formulations, the Wadley method was employed. The results showed that the synergistic ratios (SR) of the crude extract combined with pyraclostrobin and captan reached 3.70 and 2.48, respectively, indicating remarkable synergistic potential between the combinations. Further validation through in vitro detached leaf assays and pot experiments confirmed that the screened mixtures achieved significantly superior control efficacy against maize *curvularia* leaf spot compared to single-agent treatments, verifying their synergistic potentiation. To elucidate the underlying synergistic mechanism, electrical conductivity assay was used to assess the integrity of pathogen cell membranes. The results demonstrated that the electrical conductivity of fungal mycelia increased gradually with time after treatment with the combined agents, indicating that the mixtures exerted the strongest destructive effect on pathogen cell membranes. Furthermore, physiological and biochemical analyses of the pathogen after combined treatment revealed that compared with single application of the crude extract or chemical fungicides, the combined treatment groups (crude extract + pyraclostrobin, crude extract + captan) showed significantly reduced activities of superoxide dismutase (SOD) and peroxidase (POD), as well as decreased contents of soluble protein and reducing sugar, while the malondialdehyde (MDA) production was markedly elevated. These findings indicate that the combined formulations achieve synergistic antifungal effects by suppressing the activities of pathogen antioxidant enzymes, inhibiting the synthesis of proteins and reducing sugars, aggravating lipid peroxidation damage to cell membranes, and ultimately disrupting the metabolic homeostasis of *C. lunata*.

Declarations

Ethical approval

Not applicable.

Competing interests

The authors have no conflicts of interest to declare.

Funding

This study was financed in part by the Anhui Provincial Natural Science Foundation (2308085MC90), Science and Technology Innovation Group of Anhui Science and Technology University and Maize Germplasm Repository of Anhui Province(2023KJCXTD002).

Author Contributions

Xingyu Liu and Yuxun Hua designed the study and drafted the original manuscript. Haiming Duan contributed to the conception of the study. Li Yu was responsible for the preparation of experimental materials. Zhuangzhuang Li and Xinyu He undertook the collection and analysis of experimental data. Meng Wang and Haibing Yu revised and polished the manuscript critically. All authors read and approved the final manuscript.

Data Availability

The supporting information associated with this article can be obtained from the corresponding author upon making a reasonable request.

References

1. Erenstein, O., Jaleta, M., Sonder, K., Mottaleb, K., & Prasanna, B. M. (2022). Global Maize Production, Consumption and Trade: Trends and R&D Implications. *Food Security*, *14*(5), 1295–1319. https://doi.org/10.1007/S12571-022-01288-7
2. Zhang, Y., Ye, C., Su, Y., Peng, W., Lu, R., Liu, Y., Huang, H., He, X., Yang, M., & Zhu, S. (2022). Soil Acidification Caused by Excessive Application of Nitrogen Fertilizer Aggravates Soil-Borne Diseases: Evidence from Literature Review and Field Trials. *Agricultural Ecosystems & Environment*, *340*, 108176. https://doi.org/10.1016/J.AGEE.2022.108176
3. Moparthi, S., & Kleczewski, N. (2023). First Report of *Curvularia* Leaf Spot on Zea mays Caused by *Curvularia lunata* in North Carolina. *Plant Disease*, *107*(7), 2242. https://doi.org/10.1094/PDIS-10-22-

2306-PDN

4. Gao, S., Li, Y., Gao, J., Suo, Y., Fu, K., Li, Y., & Chen, J. (2014). Genome Sequence and Virulence Variation-Related Transcriptome Profiles of *Curvularia lunata*, an Important Maize Pathogenic Fungus. *Bmc Genomics*, *15*(1), 627. https://doi.org/10.1186/1471-2164-15-627
5. Guilherme, E. O., Giongo, M. V., Araujo, S. H., Ferreira, T. P., Moraes, C. B., Moura, W. S., & Santos, G. R. (2023). Jenipapo, Genipa americana L., Essential Oil and *Curvularia lunata* Control: Potential Mode-of-Action; Plant Immune Responses and Selectivity Against Beneficial Non-Target Organisms. *Industrial Crops and Products*, *199*, 116708. https://doi.org/10.1016/J.INDCROP.2023.116708
6. Yue, W., Xu, J., Lv, Z., Zhou, C., Wu, S., Zeng, Y., & Liu, P. (2025). Biocontrol Efficiency and the Functional Mechanisms of *Bacillus velezensis* RT-30 Against Kiwifruit Soft Rot. *Horticultural Plant Journal*. https://doi.org/10.1016/j.hpj.2024.09.009
7. Zouari, I., Jlaiel, L., Tounsi, S., & Trigui, M. (2016). Biocontrol Activity of the Endophytic *Bacillus amyloliquefaciens* Strain CEIZ-11 Against *Pythium aphanidermatum* and Purification of Its Bioactive Compounds. *Biological Control*, *100*, 54–62. https://doi.org/10.1016/j.biocontrol.2016.05.012
8. Chen, X., Wang, Y., Gao, Y., Gao, T., & Zhang, D. (2019). Inhibitory Abilities of *Bacillus* Isolates and Their Culture Filtrates Against the Gray Mold Caused by *Botrytis cinerea* on Postharvest Fruit. *Plant Pathology Journal*, *35*(5), 425. https://doi.org/10.5423/PPJ.OA.03.2019.0064
9. Jamal, Q., Cho, J. Y., Moon, J. H., & Kim, K. Y. (2017). Purification and Antifungal Characterization of Cyclo (D-Pro-L-Val) from *Bacillus amyloliquefaciens* Y1 Against *Fusarium graminearum* to Control Head Blight in Wheat. *Biocatalysis and Agricultural Biotechnology*, *10*, 141–147. https://doi.org/10.1016/j.bcab.2017.01.003
10. Korany, S. M., El-Hendawy, H. H., Soliman, E. R., & Elsaba, Y. M. (2023). Antagonistic Activity of *Bacillus atrophaeus* (MZ741525) Against Some Phytopathogenic Microorganisms. *Egyptian Journal of Botany*, *63*(2), 361–376. https://api.semanticscholar.org/CorpusID:253864090
11. Rawat, S., Tadiya, R., & Barthwal, S. (2025). Uncovering Bamboo-Associated Silicon-Solubilizing Bacteria from the Rhizosphere and Phyllosphere: Elevating Plant Development, Functional Enzyme Synthesis, and Biocontrol Against *Alternaria alternata* and *Curvularia lunata*. *Biology*, *80*, 2551–2562. https://doi.org/10.1007/s11756-025-01986-5
12. Xu, X., Wang, Y., Lei, T., Sohail, M. A., Wang, J., & Wang, H. (2022). Synergistic Effects of *Bacillus amyloliquefaciens* SDTB009 and Difenoconazole on Fusarium Wilt of Tomato. *Plant Disease*, *106*(8), 2165–2171. https://doi.org/10.1094/PDIS-12-21-2650-RE
13. Luo, F., Chen, H., Wei, W., Liu, H., Chen, Y., & Li, S. (2024). Screening of Antagonistic *Bacillus* Against Brown Rot in Dendrocalamus latiflorus and Preparation of Applying Bacterial Suspension. *Plant Pathology Journal*, *40*(1), 11–15. https://doi.org/10.5423/PPJ.OA.07.2023.0107
14. Li, Z., Li, J., Yu, M., Quandahor, P., Tian, T., & Shen, T. (2023). *Bacillus velezensis* FX-6 Suppresses the Infection of *Botrytis cinerea* and Increases the Biomass of Tomato Plants. *PLoS One*, *18*(6), e0286971. https://doi.org/10.1371/JOURNAL.PONE.0286971

15. He, X., Duan, H., Liu, X., Li, Z., Yu, L., Zhou, C., Lu, W., & Yu, H. (2025). Inhibitory Effect of *Bacillus velezensis* dhm2 on *Fusarium oxysporum* f. sp. cucumerinum and Synergistic Activity of Crude Lipopeptide Extract with Chemical Fungicides. *Agriculture*, *15*(16), 1730. https://doi.org/10.3390/AGRICULTURE15161730
16. Jiao, R., Cai, Y., He, P., Munir, S., Li, X., Wu, Y., Wang, J., Xia, M., He, P., Wang, G., Yang, H., Karunarathna, S. C., Xie, Y., & He, Y. (2021). *Bacillus amyloliquefaciens* YN201732 Produces Lipopeptides with Promising Biocontrol Activity Against Fungal Pathogen Erysiphe cichoracearum. *Frontiers in Cellular and Infection Microbiology*, *11*, 598999. https://doi.org/10.3389/FCIMB.2021.598999
17. Huang, N., Jin, X., Wen, J. T., Zhang, Y. F., Yang, X., Wei, G. Y., Wang, Y. K., & Qin, M. (2024). Biocontrol and Growth Promotion Potential of *Bacillus subtilis* CTXW 7-6-2 Against Rhizoctonia solani That Causes Tobacco Target Spot Disease. *Polish Journal of Microbiology*, *73*(1), 29. https://doi.org/10.33073/PJM-2024-004
18. Horsfall, J. G. (1945). *Fungicides and Their Action* (p. 239). Chronica Botanica.
19. Wadley, F. M. (1945). *The Evidence Required to Show Synergistic Action of Insecticides and a Short Cut in Analysis*. U.S. Department of Agriculture, Bureau of Entomology and Plant Quarantine.
20. Ons, L., Bylemans, D., Thevissen, K., & Cammue, B. P. A. (2020). Combining Biocontrol Agents with Chemical Fungicides for Integrated Plant Fungal Disease Control. *Microorganisms*, 8(12), 1930. https://doi.org/10.3390/microorganisms8121930
21. Lee, G., Choi, H., Liu, H., Han, Y. H., Paul, N. C., Han, G. H., Kim, H., Kim, P. I., Seo, S. I., Song, J., & Sang, H. (2023). Biocontrol of the Causal Brown Patch Pathogen Rhizoctonia solani by *Bacillus velezensis* GH1-13 and Development of a Bacterial Strain Specific Detection Method. *Frontiers in Plant Science*, *13*, 1091030. https://doi.org/10.3389/FPLS.2022.1091030
22. Loladze, A., Rodrigues, F. A., Toledo, F., San Vicente, F., Gérard, B., & Boddupalli, M. P. (2019). Application of Remote Sensing for Phenotyping Tar Spot Complex Resistance in Maize. *Frontiers in Plant Science*, *10*, 432168. https://doi.org/10.3389/fpls.2019.00552
23. Liu, X., Liu, H., Yin, F., Li, Y., Jiang, J., Xiao, Y., Wu, Y., & Qin, Z. (2024). Phytopathogenic Fungicidal Activity and Mechanism Approach of Three Kinds of Triphenylphosphonium Salts. *Journal of Fungi*, *10*(7), 450. https://doi.org/10.3390/JOF10070450
24. Cheng, C. W., Chen, L. Y., Chou, C. W., & Liang, J. Y. (2015). Investigations of Riboflavin Photolysis via Coloured Light in the Nitro Blue Tetrazolium Assay for Superoxide Dismutase Activity. *Journal of Photochemistry and Photobiology B: Biology*, *148*, 262–267. https://doi.org/10.1016/j.jphotobiol.2015.04.028
25. Zondo, S. N., Mohase, L., Tolmay, V., & Mafa, M. S. (2024). Elucidating β-1,3-Glucanase and Peroxidase Physicochemical Properties of Wheat Cell Wall Defense Mechanism Against Diuraphis noxia Infestation. *Journal of Visualized Experiments*, *209*, e66903. https://doi.org/10.3791/66903
26. Senthilkumar, M., Amaresan, N., & Sankaranarayanan, A. (2020). Estimation of Malondialdehyde (MDA) by Thiobarbituric Acid (TBA) Assay. *Plant-Microbe Interactions: Laboratory Techniques* (pp.

103–105). Springer US. https://doi.org/10.1007/978-1-0716-1080-0_25

27. Deans, C. A., Sword, G. A., Lenhart, P. A., Burkness, E., Hutchison, W. D., & Behmer, S. T. (2018). Quantifying Plant Soluble Protein and Digestible Carbohydrate Content, Using Corn (Zea mays) as an Exemplar. *Journal of Visualized Experiments*, *138*, 58164. https://doi.org/10.3791/58164
28. Jain, A., Jain, R., & Jain, S. (2020). Quantitative Analysis of Reducing Sugars by 3,5-Dinitrosalicylic Acid (DNSA Method). In Basic Techniques in Biochemistry, Microbiology and Molecular Biology: Principles and Techniques (pp. 181–183). https://doi.org/10.1007/978-1-4939-9861-6_43
29. Gao, J. X., & Chen, J. (2017). Involvement of a Polyketide Synthetase ClPKS18 in the Regulation of Vegetative Growth, Melanin and Toxin Synthesis, and Virulence in *Curvularia lunata*. *Plant Pathology Journal*, *33*(6), 597. https://doi.org/10.5423/PPJ.OA.04.2017.0079
30. Bisht, S., Balodi, R., Ghatak, A., & Kumar, P. (2018). Determination of Susceptible Growth Stage and Efficacy of Fungicidal Management of *Curvularia* Leaf Spot of Maize Caused by *Curvularia lunata* (Wakker) Boedijn. *Maydica*, *61*(3), 5. https://api.semanticscholar.org/CorpusID:54823587
31. Kim, B., Nguyen, M. V., Park, J., Kim, Y. S., Han, J. W., Lee, J. Y., Jeon, J., Son, H., Choi, G. J., & Kim, H. (2024). Edeine B1 Produced by Brevibacillus brevis Reduces the Virulence of a Plant Pathogenic Fungus by Inhibiting Mitochondrial Respiration. *mBio*, *15*(7), e01351–e01324. https://doi.org/10.1128/MBIO.01351-24
32. Bengyella, L., Yekwa, L. E., Waikhom, S. D., Nawaz, K., Iftikhar, S., Motloi, T. S., Tambo, E., & Roy, P. (2017). Upsurge in *Curvularia* Infections and Global Emerging Antifungal Drug Resistance. *Asian Journal of Scientific Research*, *10*(4), 299–307. https://doi.org/10.3923/ajsr.2017.299.307
33. Carmona, M., Sautua, F., Pérez-Hérnandez, O., & Reis, E. M. (2020). Role of fungicide applications on the integrated management of wheat stripe rust. Front. *Plant Science*, *11*, 733. https://doi.org/10.3389/fpls.2020.00733
34. Joe, A. D., Liu, R., Luo, X., Meng, X., Fang, X., Ding, Z., Liu, M., & Zheng, Z. (2025). Leveraging genome and transcriptome sequencing to decipher fungicide resistance mechanisms in crop pathogenic fungi: current status and prospects. *Pest Management Science*, *81*(12), 7639–7653. https://doi.org/10.1002/ps.70168
35. Chanworawit, K., Wangsoonthorn, P., & Deevong, P. (2023). Characterization of Chitinolytic Bacteria Newly Isolated from the Termite Microcerotermes sp. and Their Biocontrol Potential Against Plant Pathogenic Fungi. *Bioscience Biotechnology and Biochemistry*, *87*(9), 1077–1091. https://doi.org/10.1093/BBB/ZBAD080
36. Xie, S., Liu, J., Gu, S., Chen, X., Jiang, H., & Ding, T. (2020). Antifungal Activity of Volatile Compounds Produced by Endophytic *Bacillus subtilis* DZSY21 Against *Curvularia lunata*. *Annals of Microbiology*, *70*(1), 2. https://doi.org/10.1186/s13213-020-01553-0
37. Saleem, B., & Kandasamy, U. (2002). Antagonism of *Bacillus species* (Strain BC121) Towards *Curvularia lunata*. *Current Science*, *82*(12), 1457–1463. https://www.jstor.org/stable/24106181
38. Naz, I., Khan, R., Alam, S. S., Iqbal, O., Akram, S., Rajput, N. A., Younas, M. U., Qasim, M., Ali, I., Elsalahy, H. H., Aljowaie, R. M., Iqbal, R., & Munir, S. (2024). Unleashing the synergistic effect of

promising fungicides: a breakthrough solution for combating powdery mildew in pea plants. *Frontiers in Microbiology*, *15*, 1448033. https://doi.org/10.3389/fmicb.2024.1448033

39. Hao, J. J., Zhu, W. L., Li, Y. Q., Liu, J. Z., Ye, S. N., Sun, J., & Dong, Z. D. (2020). Efficacy and Profitability of Fungicide Use to Manage *Curvularia* Leaf Spot of Maize. *Crop Protection*, *132*, 105126. https://doi.org/10.1016/j.cropro.2020.105126
40. Adaangadi, K. C., Harlapur, S. I., Chakrasali, S., & Hadimani, B. R. (2018). Studies on Evaluation of Fungicides Against *Curvularia lunata* in Maize. *International Journal of Agricultural Sciences*, *14*(1), 225–228. https://doi.org/10.15740/HAS/IJAS/14.1/225-228
41. Wang, M., Duan, H., Zhou, C., Yu, L., Meng, X., Lu, W., & Yu, H. (2024). Synergistic Effects of Chemical Fungicides with Crude Extracts from *Bacillus amyloliquefaciens* to Control Northern Corn Leaf Blight. *Agriculture*, *14*(4), 606. https://doi.org/10.3390/AGRICULTURE14040606
42. Brito, F. S. D., Santos, J. R. P., Azevedo, V. C. R., Peixouto, Y. S., Oliveira, S. A., Ferreira, C. F., Haddad, F., Amorim, E. P., Fraaije, B., & Miller, R. N. G. (2020). Genetic Diversity and Azole Fungicide Sensitivity in Pseudocercospora musae Field Populations in Brazil. *Frontiers in Microbiology*, *11*, 99. https://doi.org/10.3389/fmicb.2020.00099
43. Wolkers, W. F., Oldenhof, H., Tang, F., Han, J., Bigalk, J., & Sieme, H. (2018). Factors Affecting the Membrane Permeability Barrier Function of Cells During Preservation Technologies. *Langmuir*, *35*(23), 7520–7528. https://doi.org/10.1021/acs.langmuir.8b02852
44. Yun, T. Y., Jing, T., Zang, X. P., Zhou, D. B., Li, K., Zhao, Y. K., Wang, W., & Xie, J. H. (2023). Antimicrobial Mechanisms and Secondary Metabolite Profiles of Streptomyces hygroscopicus subsp. *hygroscopicus* 5 – 4 Against Banana Fusarium Wilt Disease Using Metabolomics. *Frontiers in Microbiology*, *14*, 1159534. https://doi.org/10.3389/FMICB.2023.1159534
45. Yang, X. Q., Jiang, S. C., Zhang, M., Li, T. T., Jin, Z. C., Wu, X. X., & Chi, Y. G. R. (2024). Discovery of Novel Piperidine-Containing Thymol Derivatives as Potent Antifungal Agents for Crop Protection. *Pest Management Science*, *80*(10), 4906–4914. https://doi.org/10.1002/PS.8203
46. Chen, C. J., Li, Q. Q., Zeng, Z. Y., Duan, S. S., Wang, W., Xu, F. R., Cheng, Y. X., & Dong, X. (2020). Efficacy and Mechanism of Mentha haplocalyx and Schizonepeta tenuifolia Essential Oils on the Inhibition of Panax notoginseng Pathogens. *Industrial Crops and Products*, *145*, 112073. https://doi.org/10.1016/j.indcrop.2019.112073
47. Khaskheli, M. A., Nizamani, M. M., Tarafder, E., Das, D., Nosheen, S., Din, G. M. U., Khaskheli, R. A., Ren, M. J., Wang, Y., & Yang, S. W. (2025). Sustainable Management of Major Fungal Phytopathogens in Sorghum (Sorghum bicolor L.) for Food Security: A Comprehensive Review. *Journal of Fungi*, *11*(3), 207. https://doi.org/10.3390/jof11030207

Figures

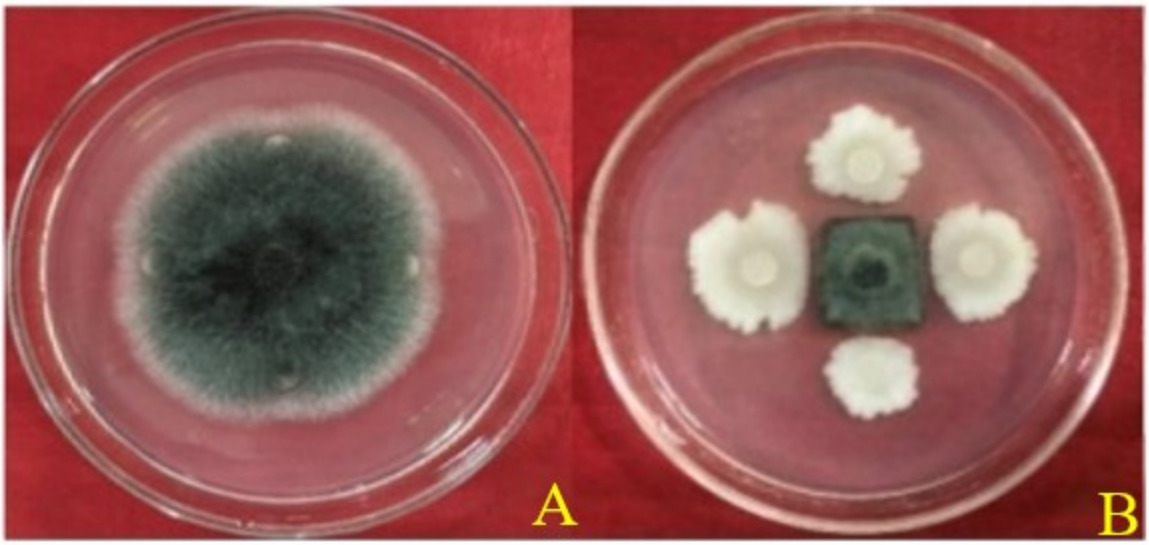


Figure 1

Inhibitory interaction observed in dual culture between biocontrol bacteria gfj-4 and *C. lunata*. Panels **A** and **B** correspond to the control of *C. lunata*and the treatment, respectively.

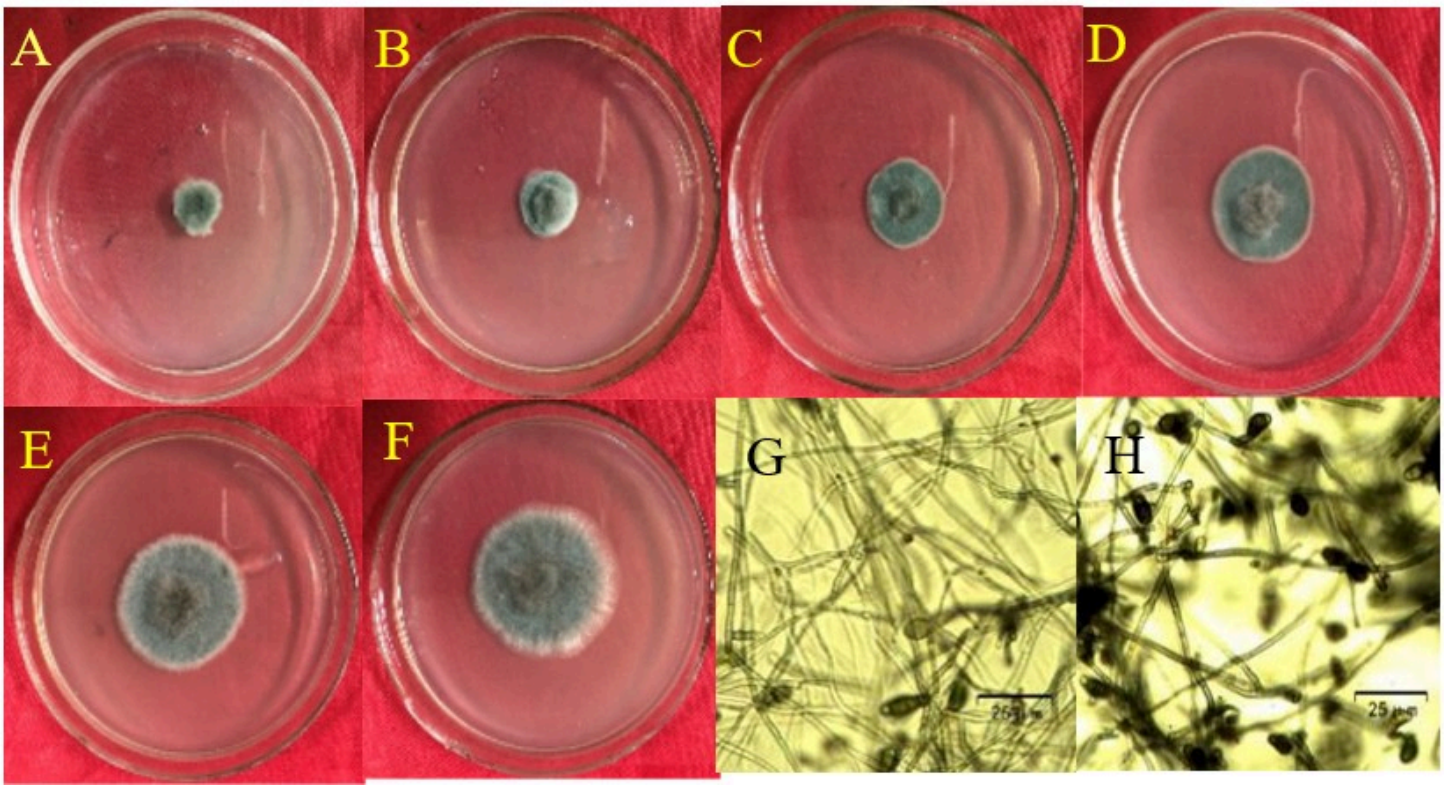


Figure 2

Inhibition effect of the crude extract on *C. lunata*. The **A, B, C, D** and **E** and **F** are 200.00, 100.00, 66.67, 50.00, 33.33 and 25.00 mg L^{-1}, respectively. **G** is the control mycelium of *C. lunata*, and H is the mycelium of *C. lunata* after treatment.

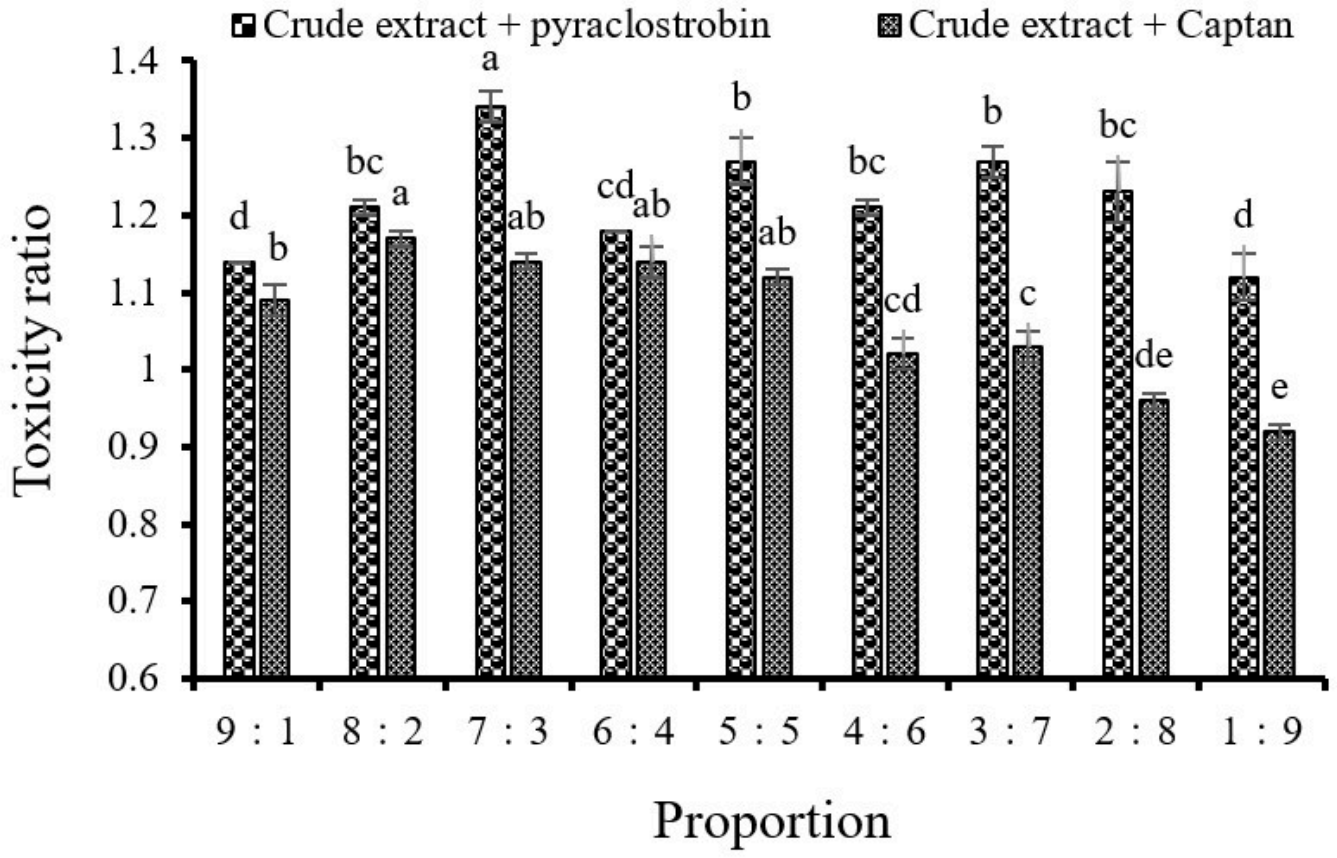


Figure 3

Toxicity potency ratios of crude extract–chemical fungicide combinations on *C. lunata*. Significant differences in toxicity ratios among various mixed ratios are indicated by distinct lowercase letters above the bars at the 0.05 significance level.

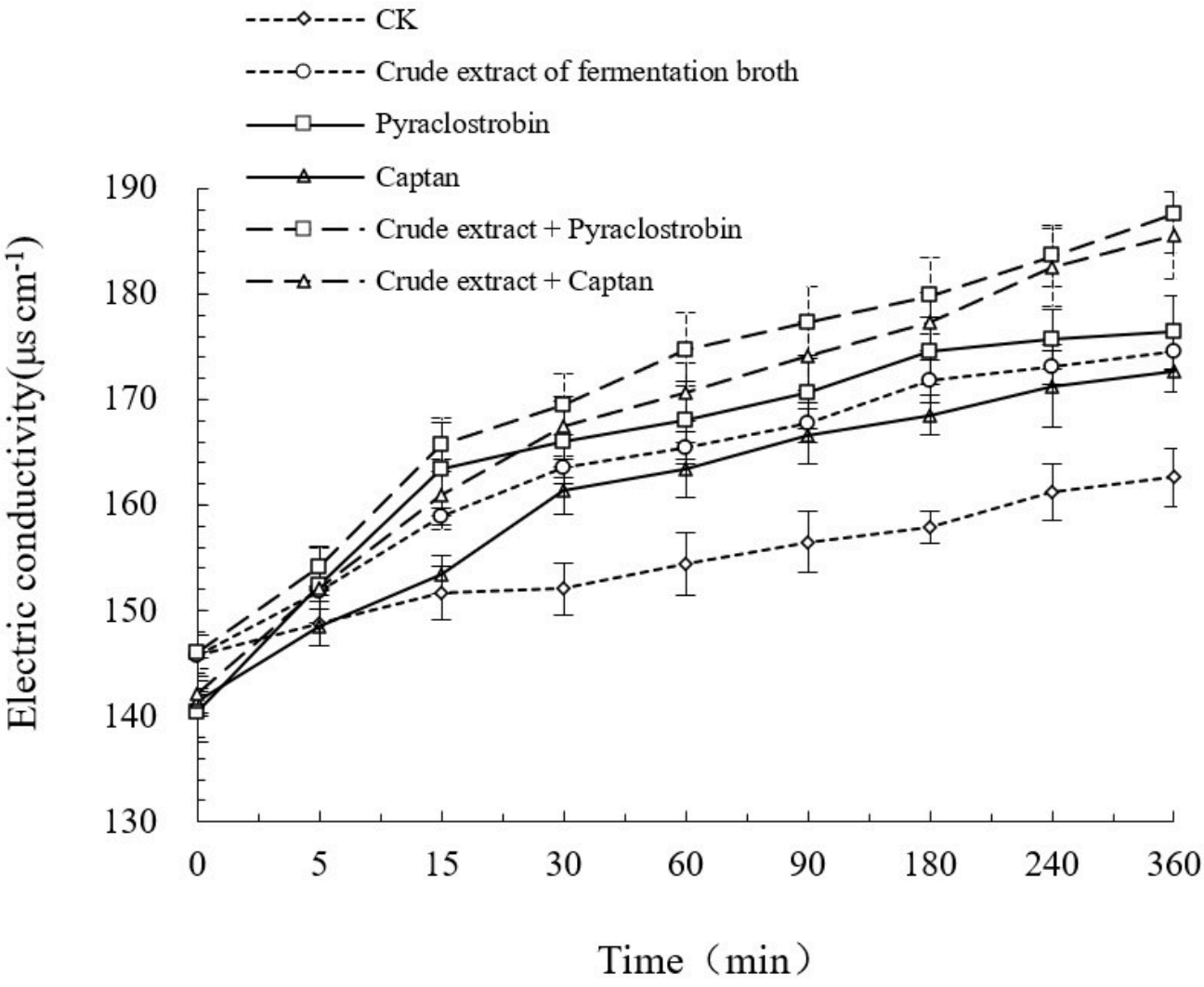


Figure 4

Influence of Synergistic Combinations on Membrane Permeability of *C. lunata*

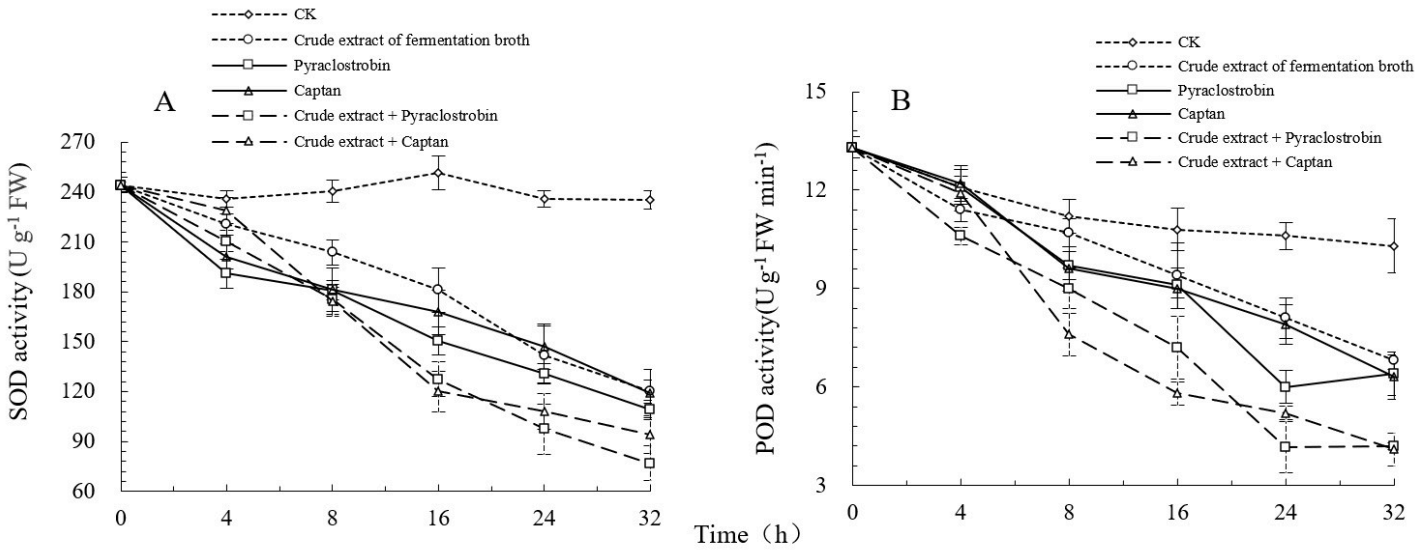


Figure 5

Effect of synergistic combination on SOD and POD activity in *C. lunata*. (**A**) and (**B**) denote the change trends of SOD and POD, respectively.

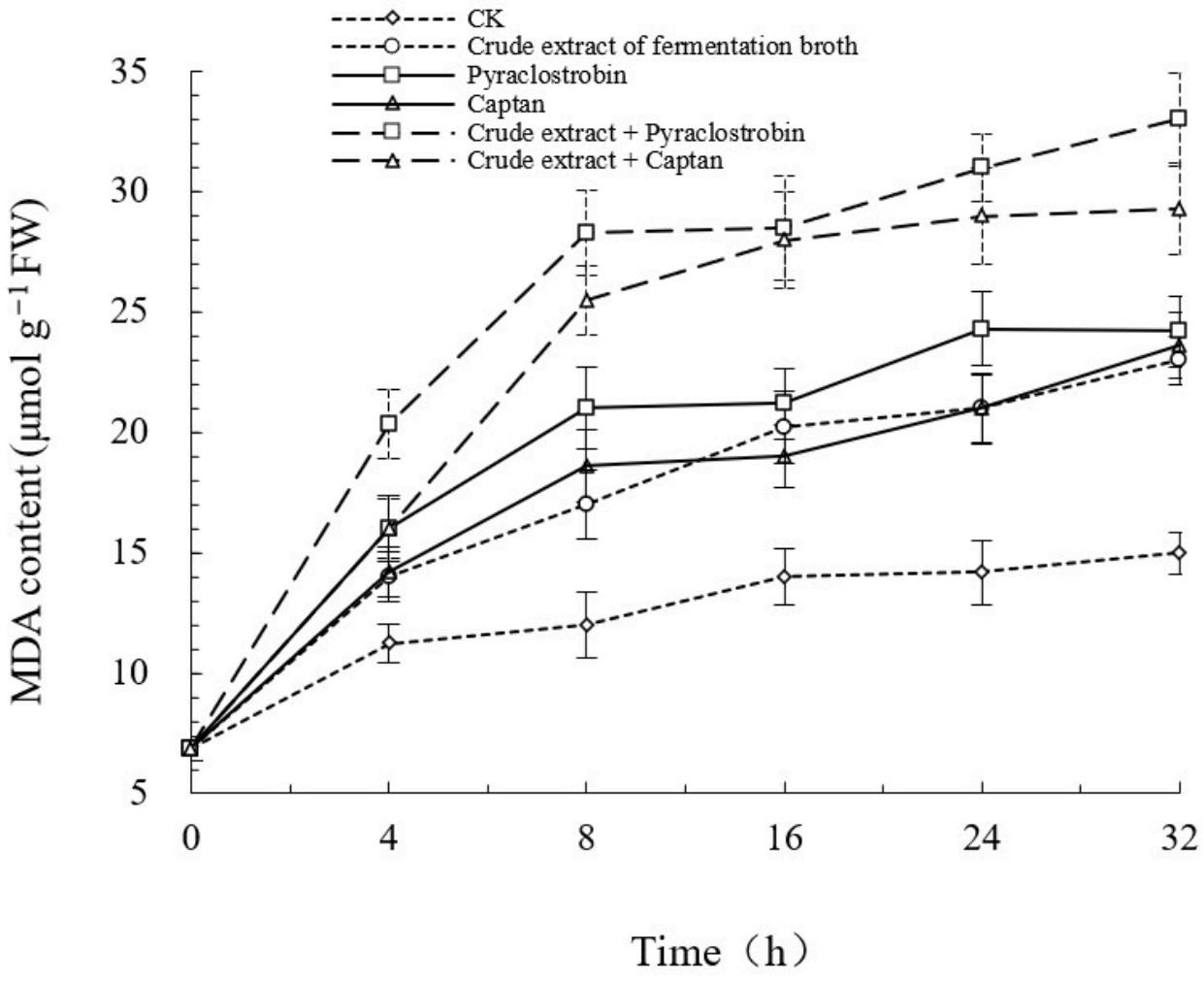


Figure 6

Effect of synergistic combination on MDA content in *C. lunata*

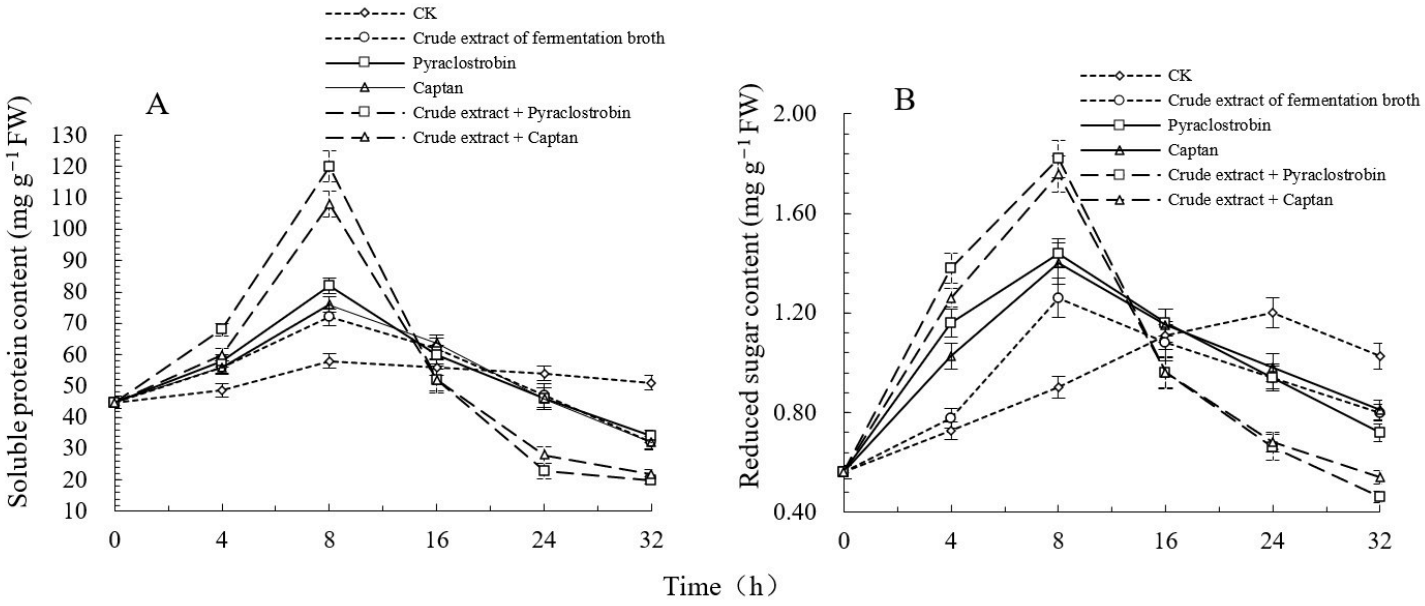


Figure 7

Effect of synergistic combination on soluble protein and reducing sugarin *C. lunata*. (**A**) and (**B**) denote the change trends of soluble protein and reducing sugar, respectively.